#### **RESEARCH PAPER**



# Synthesis, Characterization and Applications of GO-TiO<sub>2</sub> Nanocomposites in Textile Dye Remediation

V. Keerthana<sup>1</sup> · Agnishwar Girigoswami<sup>1</sup> · S. Jothika<sup>1</sup> · D. Kavitha<sup>1</sup> · A. Gopikrishna<sup>2</sup> · T. Somanathan<sup>3</sup> · Koyeli Girigoswami<sup>1</sup> ·

Received: 3 June 2021/Accepted: 14 March 2022/Published online: 27 July 2022 © The Author(s), under exclusive licence to Shiraz University 2022

#### **Abstract**

Textile azo dyes are used for coloring fabrics which are found to be potentially carcinogenic and mutagenic chemicals. It is disposed of as industrial effluents, causing major hazardous impacts on the aquatic ecosystem and getting deposited onto the soil for a prolonged period. Several conventional methods have been previously applied to eliminate these dyes but had low efficiency and high cost limitations. In order to overcome those issues, in this study, we have synthesized a GO-TiO<sub>2</sub> nanocomposite using the solvothermal method from graphene oxide (GO) nanoparticles and titanium dioxide (TiO<sub>2</sub>) nanoparticles which were synthesized individually using modified Hummer's method and sol-gel method, respectively. The prepared TiO<sub>2</sub> nanoparticles and GO-TiO<sub>2</sub> nanocomposite were characterized using UV-visible spectrophotometry, FTIR spectroscopy, dynamic light scattering, zeta potential, XRD, scanning electron microscopy, and EDAX analysis. The textile azo dyes used were Crystal Violet, Brilliant Green, Malachite Green, and Rhodamine B, and their photocatalytic degradation was observed spectrophotometrically using TiO<sub>2</sub> nanoparticles and GO-TiO<sub>2</sub> nanocomposite. From the results obtained, we found that the GO-TiO<sub>2</sub> nanocomposite was successfully synthesized with TiO<sub>2</sub> doping and effectively reduced all the dyes used in this study compared to the standard photocatalyst TiO<sub>2</sub>. On the other hand, the Brilliant Green and Malachite green have shown an increase in their color after TiO<sub>2</sub> treatment, which was diminished by using GO-TiO<sub>2</sub> nanocomposites. The biocompatibility of this GO-TiO<sub>2</sub> was studied using zebrafish embryos and the results demonstrated that the GO-TiO<sub>2</sub> nanocomposite was safe for the embryos without causing any delay in hatching or developmental abnormality. The outcome of this study yields a novel application of GO-TiO<sub>2</sub> nanocomposite in the reduction in azo dyes showing potential applications in wastewater remediation. Further studies are required to test the biocompatibility and efficacy of other dye removals.

Keywords Textile dyes removal · Wastewater remediation · Nanotechnology · Graphene oxide · Titanium dioxide

#### 

- Medical Bionanotechnology, Faculty of Allied Health Sciences, Chettinad Hospital and Research Institute, Chettinad Academy of Research and Education, Chettinad Health City, Kelambakkam 603103, Tamil Nadu, India
- Medical Biotechnology, Faculty of Allied Health Sciences, Chettinad Hospital and Research Institute, Chettinad Academy of Research and Education, Chettinad Health City, Kelambakkam 603103, Tamil Nadu, India
- Department of Chemistry, School of Basic Sciences, VISTAS, Chennai 600117, Tamil Nadu, India

#### 1 Introduction

In recent times, there is rapid industrialization and urbanization. The balance between environmental pollutants and the health of flora and fauna as well as humans have been at stake (Desai et al. 2021). Compared to all types of ecological pollutants the most severe problem is water pollution because the effluents from various dye industries meet the water bodies and contaminate them. Pigment manufacturing, food industries, cosmetic industries, textile industries, printing, leather industries, dyeing, etc., are all among the major contributors to wastewater pollution (Al-Musawi et al. 2022; Amini et al. 2008). It has been projected that 15% of the total used textile dyes remain



unreacted and contribute directly to the effluents (Yaseen and Scholz 2019; Vedhantham et al. 2022). The synthetic textile dyes contribute to water and soil contamination as released from different sources (Nelson and Hites 1980). These dye contaminants cannot be removed by ordinary treatment processes and eventually stay in the environment for many years. Their presence affects the living beings of the ecosystem, severely causing skin irritation, nausea, liver and kidney damage, vomiting, gastrointestinal (GI) tract irritation, etc., in animals and humans. They can also inhibit germination of seeds, alter the length of root and shoot in plants, and inhibit microbial activity (Mittal et al. 2010; Senthilkumaar et al. 2006).

For the management of discharge of azo dyes used in textile industries and allied industries into the soil and water bodies, many dye degradation processes have been proposed so far, which may harm the biota of the contaminated soil or water (Lellis et al. 2019). The use of nanoparticles is one of them which can ensure a sensitive way of textile dye reduction. For water decontamination, TiO<sub>2</sub> is utilized due to its photocatalytic property and advantages of being highly stable, low cost, efficient, and less toxic, whereas disadvantages are rapid recombination of excited electrons and holes, light absorption is limited within UV spectrum due to high bandgap. To overcome these limitations, several graphene-based carbon-TiO<sub>2</sub> nanocomposites were used because after exposure to UV-Visible light, the stability and photocatalytic reaction were enhanced many folds for such nanocomposites compared to only TiO<sub>2</sub> (Jeyasubramanian et al. 2019; Tayel et al. 2018). Graphene has become an interesting material in the research world with exceptional physiochemical, electrical, and optical properties that can be used in various applications, such as biosensors, catalysts, drug delivery systems, nanoelectronics, intercalating substance, polymer-based composites, for the production of hydrogen and storage (Obodo et al. 2019; Zindani and Kumar 2019; Elazab et al. 2019). TiO<sub>2</sub> is another highly studied nanoparticle for its efficient semiconductor photocatalytic activity. The environmental pollutants get degraded into fine organic chemicals using TiO<sub>2</sub> (Ram et al. 2012). Thus, both the TiO<sub>2</sub> and graphene were integrated into nanocomposite hybrids with outstanding properties for the development of novel applications. The earlier study confirmed the improved photocatalytic reactions of carbon-based TiO<sub>2</sub> composites of fullerenes, activated carbon, carbon nanotubes than only TiO<sub>2</sub>. Limitations were also present regarding the photocatalytic performance of TiO2 along with poor synthesis methods that affected the recycling of the photocatalyst and lower capacity to capture light at the site of reaction. Therefore, the carbon allotrope graphene with increased surface area (2600 m<sup>2</sup>/g), electron mobility, and transparency were highly sensible than combining other allotropes of carbon (Zhang et al. 2010a).

Metal oxide nanoparticles have been used in biomedical sciences like catalysis, biosensing, and degradation of amyloids, especially the zinc oxide nanoparticles and nanoflowers (Girigoswami et al. 2015, 2019; Akhtar et al. 2017). There is no available nanocomposite based on graphene oxide (GO) incorporated with a photocatalyst, which can degrade the textile dyes effectively and is biocompatible. In a previous study, graphene oxide has been successfully synthesized using agro wastes (Somanathan et al. 2015). In the present study, we have synthesized GO-TiO<sub>2</sub> nanocomposite and characterized them using different tools-UV-visible spectrophotometer, particle size analyzer (DLS), scanning electron microscope (SEM), Fourier-transform infrared spectroscopy (FTIR). The different azo dyes like crystal violet (CV), brilliant green (BG), malachite green (MG), and rhodamine B (RB) were studied for their reduction with the synthesized nanocomposite. Standard photocatalyst TiO<sub>2</sub> nanoparticles (NPs) were taken as a positive control. Compared to the standard photocatalyst, our synthesized nanocomposite exhibited superior remediation of textile dyes. Moreover, it was found that the synthesized nanocomposite was highly biocompatible as observed by the zebrafish embryo study.

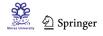
#### 2 Materials and Methods

#### 2.1 Materials

Graphite powder was procured from Sigma Chemicals, ethanol, sulfuric acid, potassium permanganate, hydrogen peroxide, hydrochloric acid, isopropanol, acetic acid, titanium tetra isopropoxide were purchased from HiMedia.

### 2.2 Synthesis of Titanium Dioxide Nanoparticles

Titanium dioxide nanoparticles (TiO<sub>2</sub> NPs) were prepared according to Venkatachalam et al. (2007) with slight modifications. To prepare TiO<sub>2</sub> NPs, 5.2 ml of isopropanol and 2.5 ml of acetic acid were mixed, and stirred for 15 min using a magnetic stirrer in a 100-ml glass beaker covered with aluminum foil to avoid evaporation of solvents. 2.5 ml of titanium tetra isopropoxide was added dropwise and stirred for 10 min further followed by the addition of 1.75 ml of deionized water (DIW). This mixture was stirred for 10 min which led to the gel formation. The contents were transferred to a porcelain crucible and kept over the hot plate for drying. Due to the calcination, the gel was converted into a yellowish precipitate. The precipitate was then crushed with mortar pestle to produce TiO<sub>2</sub> NP powder and further calcinated at 200 °C for 2 h.



# 2.3 Synthesis of Graphene Oxide (GO) from Graphite Powder

Graphene oxide (GO) nanosheets were prepared by modified Hummer's method from graphite powder as described by Zaaba et al. (2017) with slight modifications. 27 ml of sulfuric acid (H<sub>2</sub>SO<sub>4</sub>) and 3 ml of phosphoric acid (H<sub>3</sub> PO<sub>4</sub>) in a 9:1 ratio were mixed and stirred for several minutes in a 250-ml glass beaker kept on an ice bath. Then, 0.225 g of graphite powder was added into the mixing solution under stirring conditions. The solution was stirred further 10 min for proper mixing of the graphite powder and then 1.32 g of potassium permanganate (KMnO<sub>4</sub>) was added very slowly into the solution. This mixture was stirred for 6 h until the solution became dark green. The elimination of the excess of KMnO<sub>4</sub> was done by adding 0.675 ml of hydrogen peroxide (H<sub>2</sub>O<sub>2</sub>) dropwise slowly and the solution was stirred for a further 10 min. The reaction was exothermic and was conducted on an ice bath. To wash the pellet, 10 ml of hydrochloric acid (HCl) and 30 ml of distilled water (DIW) were added and centrifuged at 8000 rpm for 10 min. Then the supernatant was decanted away, and the residue was rewashed with the only DIW 3 times using the same conditions of centrifugation. The washed GO solution was dried using a hot air oven at 90 °C for 24 h to produce the GO powder.

# **2.4** Synthesis of Graphene Oxide-Titanium Dioxide Nanocomposite (GO-TiO<sub>2</sub>) Nanocomposite

The synthesized GO nanosheets were utilized to synthesize GO–TiO<sub>2</sub> nanocomposite according to Zhang et al. (2010a) with slight modification, where they have synthesized graphene–TiO<sub>2</sub>, not GO–TiO<sub>2</sub>. 0.450 g of GO as-synthesized was ultrasonicated in a 60 ml DIW and 30 ml of anhydrous ethanol solution to disperse it well, and 0.6 g of TiO<sub>2</sub> as-synthesized was added to the GO solution. The solution was stirred vigorously for 2 h to obtain a homogeneous suspension. Then, this suspension was autoclaved in a Teflon-coated autoclave and maintained at 120 °C for 24 h. The composite was recovered by filtration, washed with DIW 3 times at 8000 rpm for 10 min, and thoroughly dried at 60 °C in a hot air oven at 80 °C to get the final GO–TiO<sub>2</sub> nanocomposite.

# 2.5 Characterization of the Synthesized Nanostructures Using Different Photophysical Tools

The synthesized TiO<sub>2</sub> NPs, GO nanosheets and GO-TiO<sub>2</sub> nanocomposites were characterized using various tools.

The hydrodynamic diameter and stability in water of the synthesized GO nanosheets and GO-TiO2 nanocomposites were measured using Malvern zeta sizer according to Girigoswami et al. (2015). Briefly, the samples were diluted in 3 ml DIW and sonicated two times for 15 min to measure the hydrodynamic diameter as well as zeta potential of the synthesized nanostructures. Fourier-transform infrared spectroscopy (FTIR) technique is utilized for obtaining an infrared (IR) spectrum when the IR light falls on the sample (solid, liquid, or gas) and either gets absorbed or transmitted. FTIR is used mainly to identify compounds and molecular groups of organic compounds because they have a wide range of functional groups, crosslinks, and side chains involved. All these groups possess characteristic vibrational, stretching, and bending frequencies in the range of IR. The FTIR for GO nanosheets and GO-TiO<sub>2</sub> nanocomposite was conducted according to Girigoswami et al. (2015). The GO and GO-TiO<sub>2</sub> nanocomposites were made into pellets using KBr and the pellets were used to record the FTIR in transmittance mode. The absorption spectrum using Shimadzu UV-visible spectrophotometer was also recorded for the synthesized nanostructures according to Girigoswami et al. (2015), by diluting the samples in DIW, sonicate them, and recording the absorbance against appropriate blank solutions. High-resolution SEM (HR-SEM) is used for very high magnification visualization of the surface morphology of the synthesized nanostructures. SEM image was used for the structural confirmation and the chemical composition of the samples can be analyzed qualitatively and semiquantitatively using SEM at a selected point using EDX. The SEM and EDX were done for the synthesized GO nanosheets and GO-TiO2 nanocomposite according to Deepika et al. (2018). The samples were prepared for the SEM analysis by coating a thin layer (200 Å) of GO and GO-TiO<sub>2</sub> nanocomposite over a clean aluminum foil and dried in a vacuum and dirt-free environment. The surface was as such scanned for SEM and EDX analysis. The measurements were done at a 20 nm working distance with an accelerating voltage of 15 kV using a low energy secondary electron emitting FESEM (Su6600, Hitachi, Japan). XRD analysis was also done to find the crystalline structure of the synthesized nanostructures according to Girigoswami et al. (2015). The  $2\theta$  value was taken from  $10^{\circ}$  to 90°.

#### 2.6 Textile Dye Reduction

The application of the synthesized nanocomposite (GO–TiO<sub>2</sub>) toward textile dye remediation was also studied. The reduction in the textile dyes crystal violet (CV), brilliant green (BG), malachite green (MG), and rhodamine B (RB) was analyzed by the reduction in absorption at 588 nm for



CV, 624 nm for BG, 617 nm for MG and 553 nm for RB, respectively, using UV–visible spectrophotometer. The dye reduction was compared with standard dye reduction photocatalyst  $\text{TiO}_2$  nanoparticles (NPs). The concentration and absorption maxima ( $\lambda_{\text{max}}$ ) of the dyes in water used are given in Table 1. The concentrations of the dyes were standardized to obtain an absorbance within 0.1.

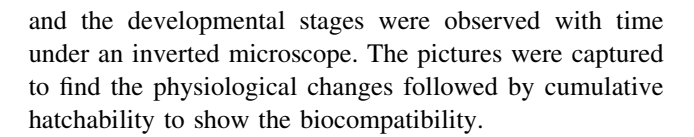
For each type of dye used namely crystal violet (CV), brilliant green (BG), malachite green (MG), and rhodamine B (RB), three tubes were taken. To each tube, 5 ml dye was added at the concentrations given in Table 1. Then, to tube 1 nothing was added, tube 2 standard photocatalyst TiO<sub>2</sub> NPs were added, and tube 3 synthesized GO-TiO<sub>2</sub> nanocomposite was added. The amount of TiO2 added was 0.01 g and GO-TiO2 was 0.001 g which was standardized and used for all the dyes. The solution of dye and the respective nanostructures (TiO2 and GO-TiO2) were mixed using vortex and exposed to sunlight for 15 min. After sunlight exposure, tubes 2 and 3 were centrifuged at 8000 rpm for 15 min to remove the nanoparticles. The supernatant was decanted in two fresh tubes and the absorbance was measured at the respective absorption maxima for the dyes mentioned in Table 1.

## 2.7 Biocompatibility Assay Using Zebrafish Embryos

Zebrafishes, both male and female, were maintained in separate tanks, with the conditions described by Girigoswami et al. (2015). Standard flakes and blood worms were fed to the zebrafishes for maintaining them in healthy conditions with 12 h light–dark conditions in fish tanks with continuous bubbling of air. The embryos were produced by external spawning. The day before, two males and one female were kept in spawning tanks with grids at the bottom, so that the eggs could percolate and settle at the bottom of the tank. The next day early morning, the eggs were isolated, washed several times with distilled water, and with the help of a microscope, healthy embryos were selected for the experiments. Nearly 30 embryos were taken for each group of treatment for only TiO<sub>2</sub> and GO—TiO<sub>2</sub> at two doses; low dose (0.1%) and high dose (0.2%),

Table 1 The concentration and  $\lambda_{max}$  of azo dyes used for the dye reduction study

Dye used	Concentration (µM)	$\lambda_{\text{max}}$ for the dyes (nm)
Crystal Violet	6	588
Brilliant green	10	624
Malachite Green	25	617
Rhodamine B	10	553



#### 3 Results

# 3.1 Synthesis and Characterization of the Nanoparticles and Nanocomposite

The synthesized nanoparticles and nanocomposite were characterized using various tools. The hydrodynamic diameter of synthesized GO-nanosheet (Fig. 1a) and GO-TiO<sub>2</sub> (Fig. 1b) the nanocomposite was found to be 79 nm and 93 nm, respectively. The size has increased from GO nanosheet to GO-TiO2 nanocomposite, confirming the incorporation of TiO<sub>2</sub> in GO. The zeta potential of synthesized TiO<sub>2</sub> nanoparticles (Fig. 1c), GO-nanosheet (Fig. 1d) and GO-TiO<sub>2</sub> nanocomposite (Fig. 1e) is found to be -29 mV, -20 mV, and -18 mV, respectively. The zeta potential of TiO<sub>2</sub> was highly stable after incorporation of TiO2 in GO; the stability has decreased to - 18 mV, which also represents a stable structure. The FTIR spectra for the synthesized nanocomposites showed typical characteristic bonds of C=C at 1634 cm<sup>-1</sup> and O-H at 3312 cm<sup>-1</sup>, respectively, for GO (Fig. 2a). After TiO<sub>2</sub> incorporation the C=C has shifted to 1646 cm<sup>-1</sup> (Fig. 2b). The new peak below 1000 cm<sup>-1</sup> represents the presence of Ti-O-Ti. The absorption spectra of TiO<sub>2</sub> and GO-TiO<sub>2</sub> nanocomposite are shown in Fig. 2c. We could see a typical shoulder peak of TiO<sub>2</sub> at 304 nm, whereas GO-TiO<sub>2</sub> nanocomposite has a small shoulder peak around 304 nm, confirming the incorporation of TiO<sub>2</sub> in the GO-TiO<sub>2</sub> nanocomposite. To confirm the crystalline structure of the synthesized TiO<sub>2</sub> nanoparticles and GO-TiO<sub>2</sub> nanocomposites, we have done XED analysis. The results (Fig. 2d) showed that the XRD peaks corresponding to the JCPDS pattern of TiO<sub>2</sub> anatase (JCPDS card no. 21-1272) were all present (Scarpelli et al. 2018; Awang and Talalah 2019). The TiO<sub>2</sub> XRD showed peaks at (101), (004), (200), (105), and (204), which matches with the JCPDS pattern for TiO<sub>2</sub> anatase. When GO was incorporated, the XRD peak intensity was found to be increased for each of these planes.

The surface morphology of the synthesized nanocomposite was visualized using SEM analysis. The typical nanosheet layered structure was observed for only GO (Fig. 3a). The incorporation of TiO<sub>2</sub> was visible over the GO nanosheets as seen in Fig. 3b. The size of TiO<sub>2</sub> NPs was found to be 20 nm. The EDX of GO–TiO<sub>2</sub> nanocomposite showed the incorporation of TiO<sub>2</sub> in the synthesized GO–TiO<sub>2</sub> nanocomposite with 1.2% incorporation by



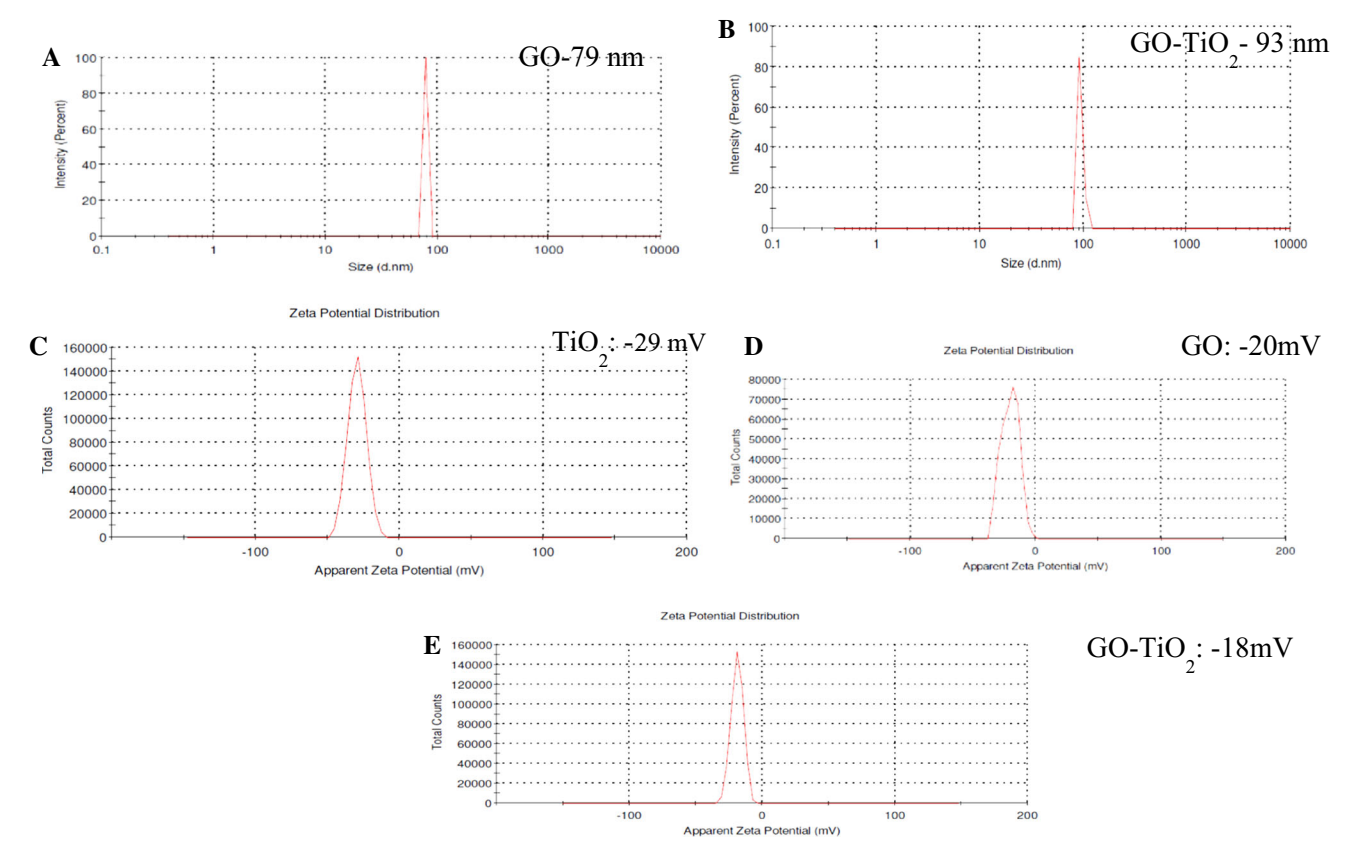


**Fig. 1** The characterization of the synthesized GO-TiO<sub>2</sub> nanocomposite. The hydrodynamic diameter of synthesized **a** GO-nanosheet and **b** GO-TiO<sub>2</sub> nanocomposite, the zeta potential of synthesized

c TiO $_2$  nanoparticles (- 29 mV) d GO nanosheet (- 20 mV) and e GO-TiO $_2$  nanocomposite (- 18 mV)

weight as shown in Fig. 3c. The peaks denote the incorporation of TiO<sub>2</sub> in the nanocomposite.

## 3.2 Textile Dye Reduction by Synthesized GO-TiO<sub>2</sub> Nanocomposite

The reduction in the absorbance as observed spectrophotometrically for the dyes CV, BG, MG, and RB using  $TiO_2$  NPs and  $GO-TiO_2$  nanocomposites is shown in Fig. 4a, c, e, g, respectively. The change in the color of the dyes after the addition of  $TiO_2$  NPs and  $GO-TiO_2$  nanocomposites for CV, BG, MG, and RB is shown in Fig. 4b, d, f, and h, respectively. The absorption spectrum of the textile dyes without any catalyst and without any exposure to irradiation is shown in Fig. 4i. The spectrophotometric observation clearly showed that after treatment with  $GO-TiO_2$  nanocomposites, all the CV, BG, MG, and RB dyes exhibited a complete reduction in the  $\lambda_{max}$ , respectively.

### 3.3 Biocompatibility Assay

The zebrafish embryos were taken as an in vivo model to study the biocompatibility of the synthesized

nanostructures. TiO2 and GO-TiO2 nanocomposite were compared, and the results are depicted in Fig. 5. The pictures were taken at 54 h post-fertilization (hpf) and the experiments were repeated thrice. The images showed that the control embryos had a transparent medium, and they were 100% hatched after 72 hpf (Fig. 6). In the TiO<sub>2</sub>treated zebrafishes, there was an aggregation of nanoparticles above the embryos, which may cause hindrance for the exchange of essential nutrients and gases required for their growth and development. This may be the reason for the delayed hatching of the embryos after treatment with the only TiO<sub>2</sub> at a high dose, and there was only 96% hatching compared to 100% observed in other treatments. The embryos treated with low as well as a high dose of GO-TiO<sub>2</sub> had some aggregation on the egg surface, but it was less pronounced compared to only TiO<sub>2</sub> nanoparticles. There was delayed hatching observed for GO-TiO<sub>2</sub> at a high dose, but the effect was lower compared to only TiO<sub>2</sub> treatment, and 100% hatching was observed for both low as well as a high dose of GO-TiO<sub>2</sub> treatment.



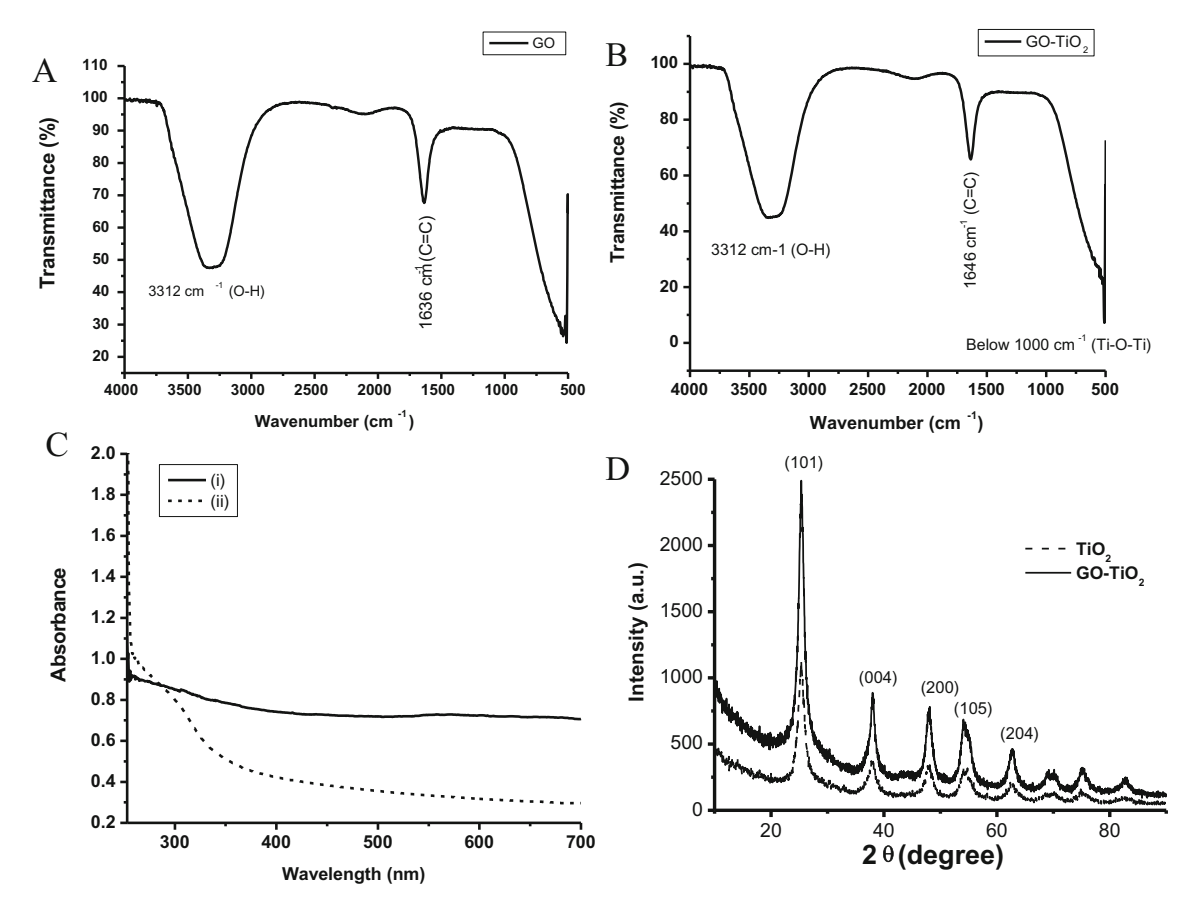


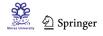
**Fig. 2** The FTIR spectra of synthesized **a** GO nanosheet and **b** GO—TiO<sub>2</sub> nanocomposite. **c** The UV–visible absorption spectrum of (i) GO–TiO<sub>2</sub> nanocomposite (solid line) and (ii) TiO<sub>2</sub> nanoparticles

(dashed) **d** The XRD spectrum of (i) GO–TiO<sub>2</sub> nanocomposite (solid line) and (ii) TiO<sub>2</sub> nanoparticles (dashed)

#### 4 Discussion

Titanium dioxide nanoparticles (TiO<sub>2</sub>) are a well-known widely used photocatalyst to reduce numerous pollutants and chemicals such as textile azo dyes into non-toxic residues. In recent studies, the two-dimensional Graphene oxide (GO) nanosheets exhibited astonishing properties mainly in visible light response and enhanced photocatalytic activity. Moreover, by doping TiO<sub>2</sub> nanoparticles onto the GO nanosheets forming Graphene oxide-Titanium dioxide (GO-TiO2) nanocomposite, which was found to be a promising semiconductor photocatalyst under the visible light spectrum. The nanocomposite exhibited overall visible light response, enhanced bandgap reduction, surface plasmon resonance, electron mobility, and reduced electron-hole recombination. So far, the application of GO-TiO<sub>2</sub> nanocomposite was studied only for volatile aromatic pollutants (Zhang et al. 2010a), but its application in reducing toxic textile dyes has not been explored. We have successfully synthesized and characterized TiO<sub>2</sub> nanoparticles, GO nanosheets, and GO-TiO2 nanocomposite. To achieve a maximum photocatalytic reduction in azo dyes such as Crystal Violet, Brilliant Green, Malachite Green, and Rhodamine B, the dyes were simulated with water, treated simultaneously with only TiO<sub>2</sub> nanoparticles, and GO–TiO<sub>2</sub> nanocomposite, and was monitored for their reduction. Previous studies exist for the application of TiO<sub>2</sub>–graphene nanocomposites for the decontamination of wastewater (Tayel et al. 2018).

TiO<sub>2</sub> nanoparticles were synthesized successfully, using TTIP as a precursor through sol–gel method. The characterizations were executed after drying and calcination at 200 °C for 2 h. The particle size of the synthesized TiO<sub>2</sub> NPs was found to be around 20 nm (Fig. 3b) and was also very highly stable as observed from the zeta potential value of – 29 mV (Fig. 1c). The smaller the size, the activity of the nanoparticles is higher due to the very high surface area to volume ratio. The characteristic absorption spectrum with a typical shoulder peak was also observed for the synthesized TiO<sub>2</sub> NPs at 304 nm (Fig. 2c). Researchers have shown a similar kind of shoulder peak obtained after TiO<sub>2</sub> NP synthesis using the sol–gel method (Venkat-achalam et al. 2007). These characterizations of TiO<sub>2</sub> NPs



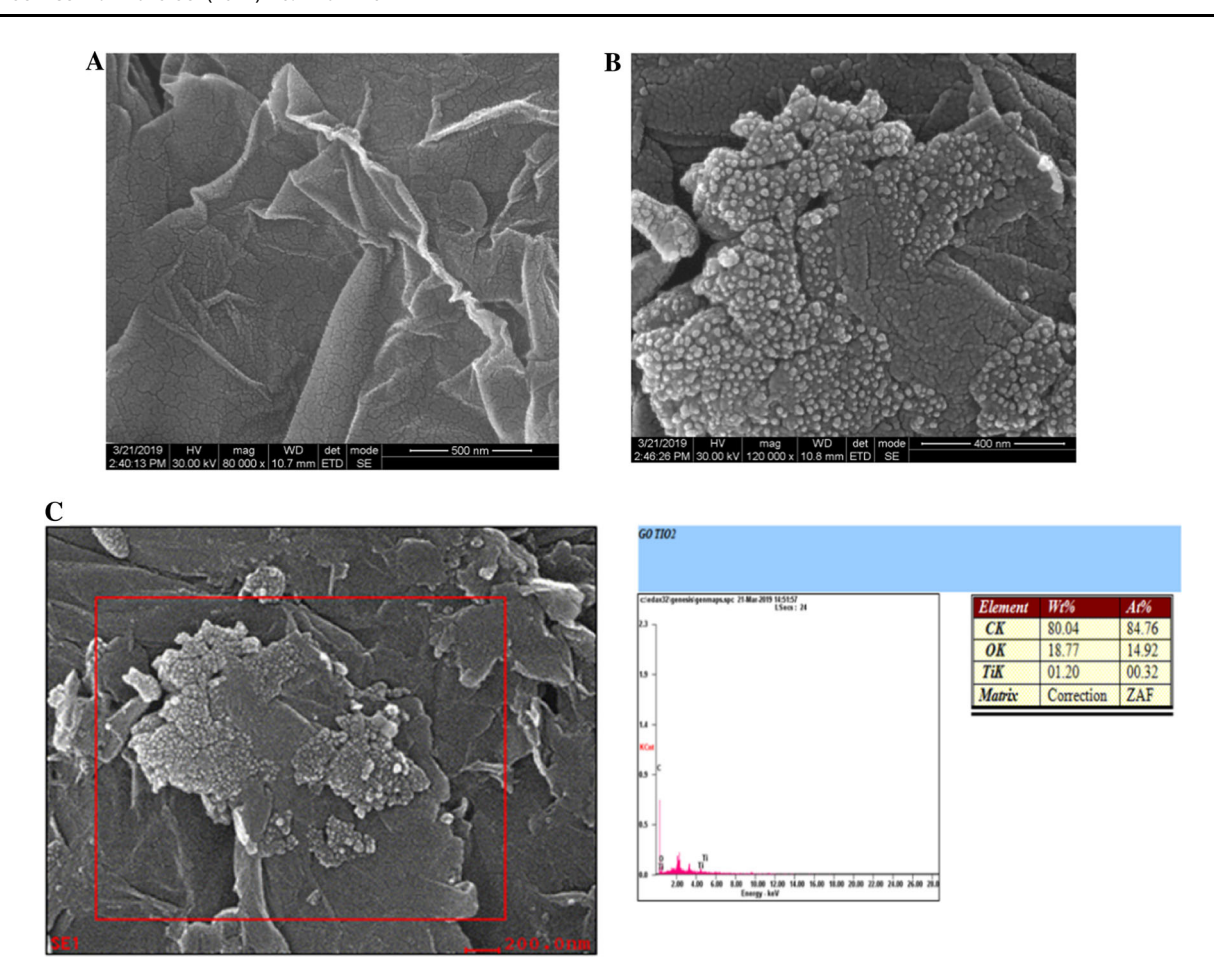


**Fig. 3** The scanning electron microscope (SEM) images of **a** GO nanosheets and **b** GO–TiO<sub>2</sub> nanocomposite. This visualizes the GO sheet formation and further incorporation of TiO2 into GO sheets.

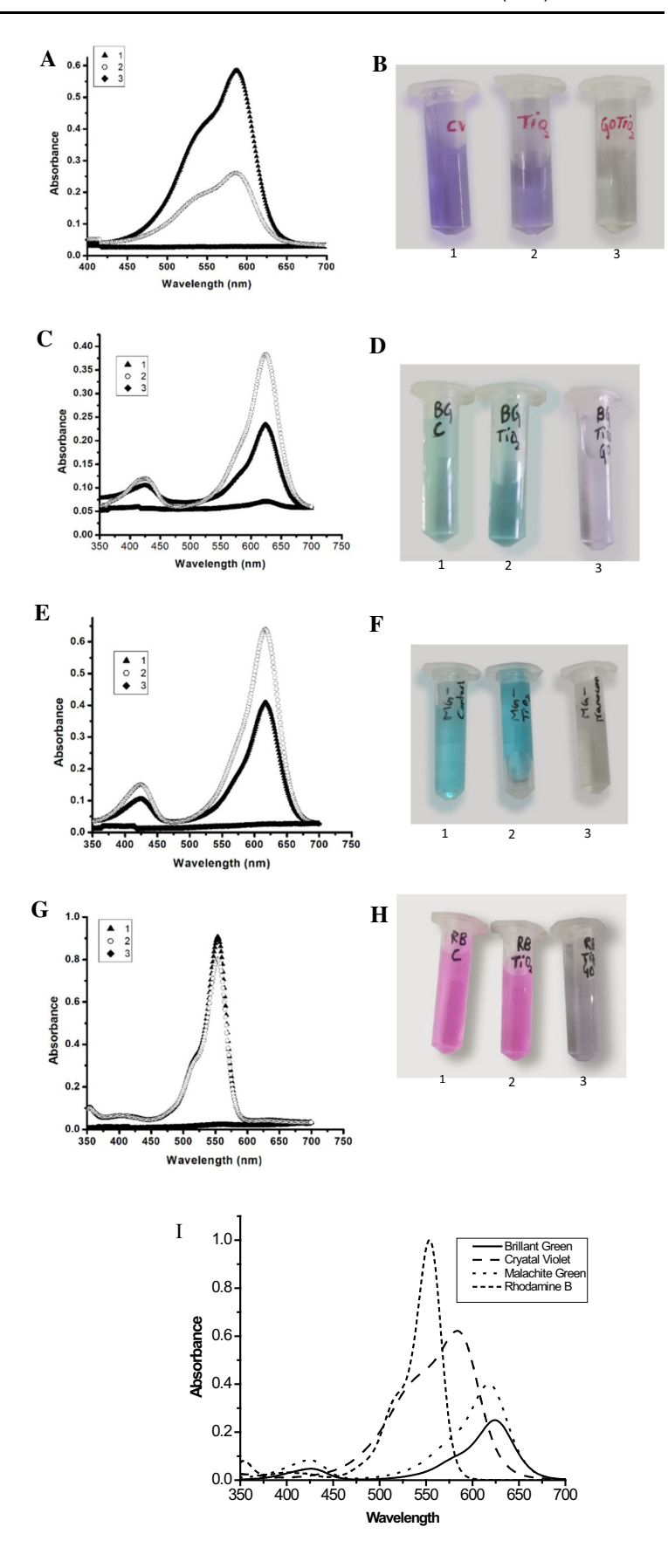
c The EDX analysis of GO-TiO<sub>2</sub> nanocomposite. This gives the exact composition of the GO-TiO<sub>2</sub> nanocomposite

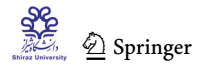
showed that the synthesis was successful and the particles are highly stable in water.

To further proceed toward the nanocomposite synthesis, we have synthesized GO from graphene using modified Hummer's method. The GO was synthesized successfully as evidenced from the FTIR spectrum, which shows the characteristic bond vibrations for C=C at 1634 cm<sup>-1</sup> and O-H at 3312 cm<sup>-1</sup>, respectively, for GO (Fig. 2a) as well as surface morphology visualized through SEM analysis (Fig. 3a). The typical layered structure of GO is observed in the SEM analysis. The synthesized GO was utilized to synthesize GO-TiO2 nanocomposite using the hydrothermal method and characterized for the parameters. The FTIR spectroscopy showed that additional bands for Ti-O-Ti were incorporated in the spectrum apart from a shift in C=C to 1646 cm<sup>-1</sup> from 1632 cm<sup>-1</sup> (Fig. 2b). To further confirm the TiO<sub>2</sub> incorporation, SEM and EDX analysis was done. The SEM image clearly shows the incorporation of TiO<sub>2</sub> NPs on the surface of the GO sheets (Fig. 3b). Further, the EDX analysis (Fig. 3c) showed peaks corresponding to carbon, oxygen, and titanium. Thus, the incorporation of TiO2 NPs in the GO sheets has been confirmed. The XRD pattern of TiO2 and GO-TiO2 is shown in Fig. 2d. The graph shows that the nanoparticles were successfully synthesized, and the XRD peaks corroborate with the JCPDS pattern (card number 21-1272) for anatase TiO<sub>2</sub> nanoparticles. After GO incorporation, the intensity of each peak has increased. In previous study, researchers have shown that similar peaks were obtained for TiO<sub>2</sub> anatase (Scarpelli et al. 2018; Awang and Talalah 2019). It is known that if TiO<sub>2</sub> is incorporated in GO nanosheets, the photocatalytic activity will be enhanced. The improvement in photocatalytic activity is attributed to the following schemes: (i) the two-dimensional matt structure of GO will enhance the surface area of TiO<sub>2</sub> after the interaction. (ii) The  $\pi$ - $\pi$  interaction between the aromatic contaminants and the network of aromatic groups of GO increases the adsorption of the contaminants to the nanocomposite facilitating the photocatalytic reduction and (iii) the nanocomposite decreases the recombination of the holes (positive) with the photogenerated electrons, because GO is a conductor of electrons and it acts as a sink for



Fig. 4 The textile dyes reduction by the GO-TiO<sub>2</sub> nanocomposite. The symbols used are: 1-only dye, 2-dye with TiO<sub>2</sub>, 3—dye with GO-TiO2 nanocomposite for all the graphs (a, c, e, g) and all the figures (b, d, f, h). The reduction in a Crystal Violet (CV), c Brilliant Green (BG), e Malachite Green (MG), and g Rhodamine B (RB), respectively, using GO-TiO<sub>2</sub> nanocomposite studied spectrophotometrically. The reduction in **b** CV, **d** BG, **f** MG, and h RB dye visible in the tubes. i The absorbance spectra of the dyesCrystal Violet (CV), Brilliant Green (BG), Malachite Green (MG), and Rhodamine B (RB) without the presence of any catalyst and without any sunlight exposure





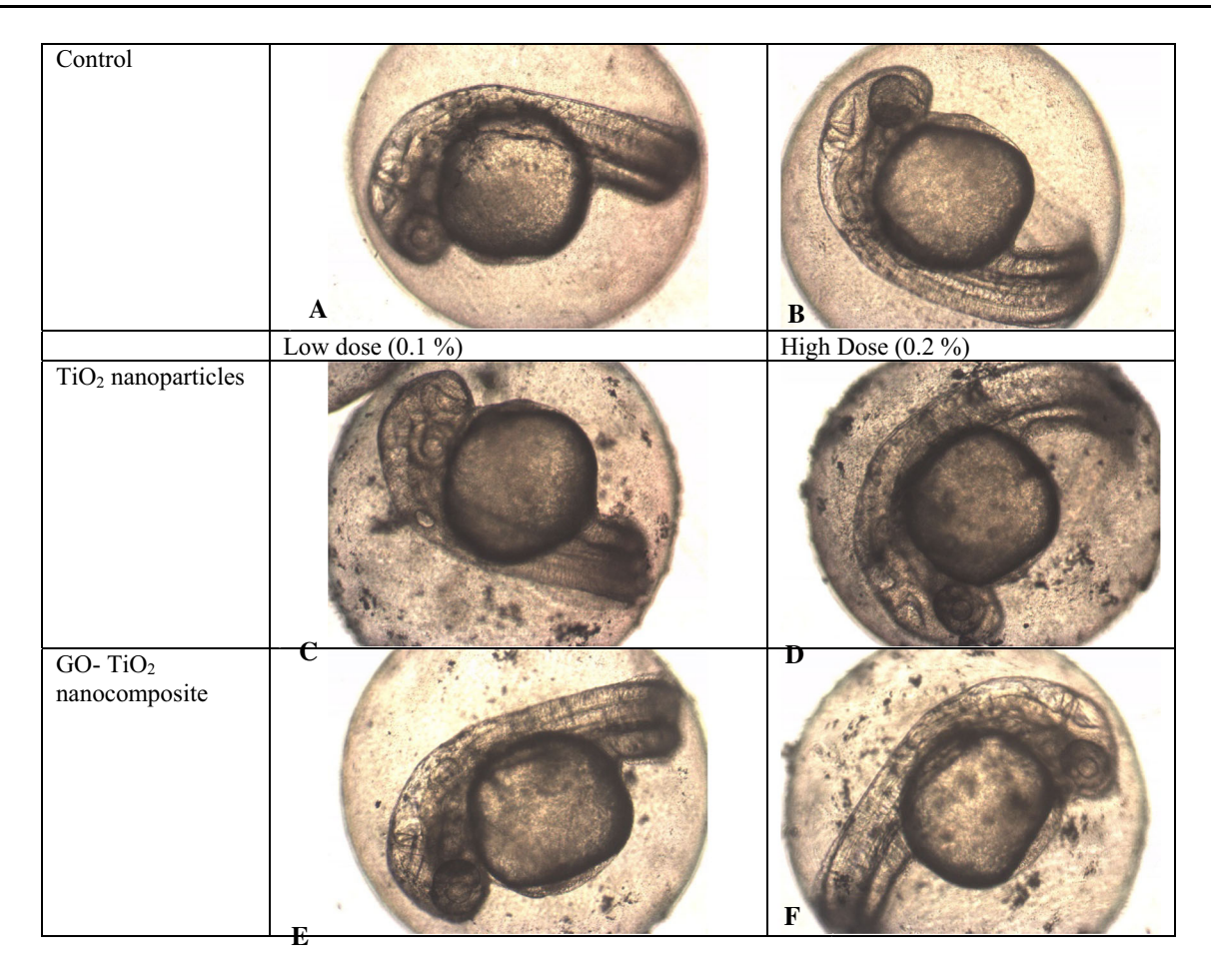


Fig. 5 The zebrafish embryos at 54 hpf in control (a) and (b), and after treatment with  $TiO_2$  (0.1%) (c),  $TiO_2$  (0.2%) (d),  $GO-TiO_2$  (0.1%) (e) and  $GO-TiO_2$  (0.2%) (f)

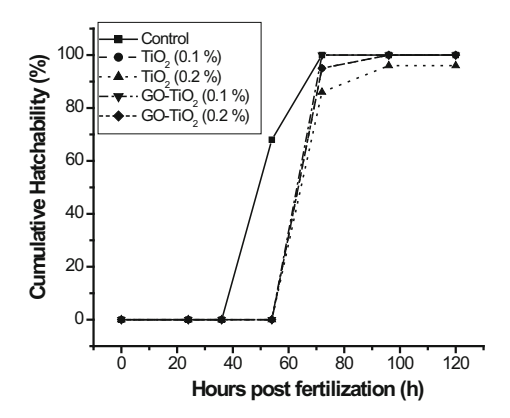


Fig. 6 Cumulative hatchability of zebrafish embryos at different hpf after treatment with TiO<sub>2</sub> and GO–TiO<sub>2</sub> nanoparticles

photogenerated electrons generated on the  $TiO_2$  surface (Zhang et al. 2010b; Yoo et al. 2011; Liu et al. 2010; Leary and Westwood 2011).

The photocatalytic activity of the  $GO-TiO_2$  nanocomposite was applied for the reduction in textile dyes—crystal violet (CV), brilliant green (BG), malachite green (MG),

and rhodamine B (RB). The reduction in CV was done using the nanocomposite as well as TiO<sub>2</sub> NPs. The effect in decolorization of CV was monitored spectrophotometrically using TiO<sub>2</sub> NPs (0.001 g) GO-TiO<sub>2</sub> (0.01 g) as shown in Fig. 4a and the percentage of reduction is shown in Table 2. The GO-TiO<sub>2</sub> nanocomposite could reduce 95% of the dye compared to the only TiO2, which was 47%. Although there is no peak intensity observed at  $\lambda_{\text{max}}$ of CV (588 nm) after GO-TiO<sub>2</sub> nanocomposite treatment and the solution has also become colorless, showing complete dye remediation (Fig. 4b). GO-TiO<sub>2</sub> nanocomposite could reduce the BG dye completely as visible from the absence of any absorption peak at 624 nm ( $\lambda_{max}$  of BG) (Fig. 4c). TiO<sub>2</sub> was found to increase the intensity of the dye instead of reducing it. We got a similar finding for another green dye MG, which we will discuss next. The percentage of BG reduced by TiO<sub>2</sub> NPs and GO-TiO<sub>2</sub> nanocomposites is shown in Table 2. The percent reduction is negative (- 94%) for the standard photocatalytic agent TiO<sub>2</sub>, whereas the GO-TiO<sub>2</sub> nanocomposite could reduce the dye to 81%. The color of the dye is completely reduced as shown in the picture (Fig. 4d).



Table 2 The percentage reduction in different textile dyes using TiO<sub>2</sub> nanoparticles and GO-TiO<sub>2</sub> nanocomposites

Dye used for reduction	% Reduction in dye using TiO2 nanoparticles	% Reduction in dye using GO-TiO2 nanocomposite
Crystal violet (CV)	47	95
Brilliant Green (BG)	<b>- 94</b>	81
Malachite Green (MG)	<b>–</b> 61	93
Rhodamine B (RB)	07	97

GO-TiO<sub>2</sub> nanocomposite could reduce the MG dye completely as visible from the absence of any absorption peak at 617 nm ( $\lambda_{max}$  of MG) (Fig. 4e). TiO<sub>2</sub> was found to increase the intensity of the dye instead of reducing it, similar to BG. The percentage of MG reduced by TiO<sub>2</sub> NPs and GO-TiO<sub>2</sub> nanocomposites is shown in Table 2. There was a negative reduction (-61%) i.e., increase in color of MG with standard photocatalytic agent TiO<sub>2</sub>, whereas GO-TiO<sub>2</sub> nanocomposite could reduce 93% of the dye. The absence of absorption peak at  $\lambda_{max}$  of MG showed that the dye is completely reduced by the synthesized nanocomposite which was also supported by the picture showing no color of the MG dye after GO-TiO<sub>2</sub> nanocomposite treatment (Fig. 4f). GO-TiO<sub>2</sub> nanocomposite could reduce the RB dye completely as visible from the absence of any absorption peak at 553 nm ( $\lambda_{max}$  of RB) (Fig. 4g). TiO<sub>2</sub> also reduced the dye but was not effective compared to GO-TiO<sub>2</sub> nanocomposite. The percentage of RB reduced by TiO<sub>2</sub> NPs, and GO-TiO<sub>2</sub> nanocomposites are shown in Table 2. There was minimal effect of standard photocatalyst TiO<sub>2</sub> on RB dye reduction (7%), whereas the synthesized nanocomposite could reduce 97% of the dye RB. The absence of any absorption peak at  $\lambda_{max}$  of RB after GO-TiO<sub>2</sub> nanocomposite treatment showed complete dye remediation which was also supported by the picture (Fig. 4h). The special mention requires for the dyes brilliant green (BG) and malachite green (MG), in which cases the standard photocatalytic agent TiO<sub>2</sub> increased the color intensity rather than decreasing it. Moreover, the use of synthesized GO-TiO<sub>2</sub> nanocomposite could reduce the colors of BG and MG effectively as visible from the loss of absorption peak for BG (Fig. 4c) and MB (Fig. 4e) spectrophotometrically. The absorption spectrum of the dyes crystal violet, Rhodamine B, Brilliant green, and Malachite green is shown in Fig. 4i without any catalyst and without any irradiation. The peak values show that there is no quenching of dye peaks before and after exposure to sunlight.

Methylene blue (MB) reduction has been demonstrated by other researchers using graphene– $TiO_2$  nanocomposite (Zhang et al. 2010a). Nitrogen doping with graphene  $TiO_2$  nanocomposite was also shown to improve the

photocatalytic activity for the purpose of MB dye reduction (Shi et al. 2014). Researchers have extensively reviewed the recent progress in TiO<sub>2</sub> photocatalyst coupled with graphene materials, where the objective was to extend the absorption of light of TiO<sub>2</sub> from UV wavelengths toward the visible region. The review also focused on the current advances in the design as well as applications towards the degradation of synthetic dyes through photocatalysis (Giovannetti et al. 2017). Another review discussed the recent developments involved in the chemistry of TiO<sub>2</sub>/G and TiO<sub>2</sub>/GO nanocomposites. There was a detailed report on the mechanistic fundamentals, in short, of TiO<sub>2</sub> and TiO<sub>2</sub>/G and TiO<sub>2</sub>/GO photocatalysts along with the different synthesis strategies as well as characterization techniques applied to study TiO<sub>2</sub>/G and TiO<sub>2</sub>/GO nanocomposites. A brief description of the applications of nanocomposites for water decontamination was included. Wastewater treatment application was discussed for graphene-TiO<sub>2</sub> nanocomposite, not GO-TiO<sub>2</sub> nanocomposite which is a different material from the one we have synthesized in this study. Moreover, the different doping like N<sub>2</sub> gas, SiO<sub>2</sub>, CNT addition to the G/TiO<sub>2</sub> is discussed. These doping make a different nanocomposite than what we have engineered (Tayel et al. 2018). In another study, the degradation of methyl orange (MO), an azo dye, was analyzed in simulated wastewater after treatment with the synthesized (GO–TiO<sub>2</sub>–ZnO) nanocomposite (Raliya et al. 2017). Reports also exist on the photocatalytic degradation of structurally different azo dyes (amaranth, sunset yellow, and tartrazine) utilizing TiO<sub>2</sub>-Pt nanoparticles (TPt), TiO<sub>2</sub>-Pt/graphene oxide (TPt-GO), and TiO<sub>2</sub>-Pt/reduced graphene oxide (TPt-rGO) composites in the presence of UV and natural sunlight irradiation (Rosu et al. 2017). In another study, graphene oxide (GO) flakes supported titanium dioxide nanoparticles, and SiO<sub>2</sub> insulated nano-sized magnetite aggregates were synthesized. The magnetically recyclable nanocomposite was made with SiO<sub>2</sub> assistance which was different from our nanocomposite (Linley et al. 2014). Thus, we propose that incorporating TiO<sub>2</sub> in GO might have facilitated the access to free electron, which participates in reducing the dye during photocatalysis. This



is the reason we believe that GO-TiO<sub>2</sub> is a superior photocatalyst compared to only TiO<sub>2</sub>.

To understand the biocompatibility of the synthesized nanocomposites, we have executed an in vivo experiment with zebrafish embryos (Figs. 5 and 6). The embryos were treated with different doses of TiO2 and GO-TiO2 nanoparticles (0.1 and 0.2%), and their developmental stages were monitored along with their hatchability. There was an aggregation of nanoparticles observed for TiO<sub>2</sub>treated embryos at both low and high doses, and the embryos showed delayed hatching at high dose (0.2%) of TiO<sub>2</sub>. Only 86% of embryos hatched after high dose treatment with TiO2 after 72 h, whereas 96% hatched for GO-TiO<sub>2</sub> at the same time interval at high dose. After 96 h 100% hatching was observed for GO-TiO<sub>2</sub> at high dose, but there was only 96% hatching for high dose TiO<sub>2</sub> treatment. Thus, it was observed that TiO2 at the high dose had delayed hatching as well as embryo killing effect (since 100% eggs did not hatch), and on the other hand, GO-TiO<sub>2</sub> at high dose showed 100% hatching.

The outcome of our study demonstrated that GO-TiO<sub>2</sub> nanocomposite was successfully synthesized and the nanocomposite was effective in reducing the textile dyes crystal violet (CV), brilliant green (BG), malachite green (MG), and rhodamine B (RB), although the effectiveness was different for different kinds of dyes. In the case of BG and MG, there was a complete reduction in the dyes using the nanocomposite, whereas the standard photocatalyst, TiO<sub>2</sub> NPs, alone could not reduce the dye intensity, instead enhanced it. The biocompatibility study using zebrafish embryos also showed that the synthesized GO-TiO<sub>2</sub> nanocomposite was non-toxic to the aquatic environment. However, there are previous reports on the toxicity of TiO<sub>2</sub> nanoparticles Artemisia absinthium L, which underwent salinity stress (Shariatzadeh Bami et al. 2021). In vivo reversal of TiO2 toxicity in rat spermatozoa was also observed using vitamin A and E (Khanvirdiloo et al. 2021). Thus, the dose and exposure route of TiO2 may pose some threat to the environment. Therefore, our synthesized GO– TiO<sub>2</sub> nanocomposite was very effective in reducing the dyes compared to the standard photocatalytic agent, TiO<sub>2</sub> NPs.

#### 5 Conclusion

The profound use of nanomaterials in the field of bioremediation has been evident in recent years. We attempted to synthesize GO-TiO<sub>2</sub> nanocomposite by solvothermal method and applied it to reduce textile dye. As it is well known that textile dyes are not dissociated when used for dyeing purposes and the unused dyes are rejected as effluent in the water bodies. The engineered GO-TiO<sub>2</sub> nanocomposite could effectively reduce the textile dyes namely crystal violet (CV), brilliant green (BG), malachite green (MG), and rhodamine B (RB). The dyes like MG and BG were usually not reduced by known photocatalyst, TiO<sub>2</sub> NPs, but were completely reduced by our synthesized GO–TiO<sub>2</sub> nanocomposite. The nanocomposite was reducing CV, BG, MG, and RB completely as visible from the absence of color. Further studies for the biocompatibilities of the nanocomposite need to be explored. In the future, studies are warranted using different other types of water contaminants and other textile dyes.

Acknowledgements We are grateful to the Chettinad Academy of Research and Education for providing us the necessary infrastructure and chemicals to conduct the experiments. The authors acknowledge funding from the Council of Scientific and Industrial Research (CSIR), INDIA, Scheme No. 01(2868)/17/EMR-II. We also thank Dr. Surajit Pathak for providing us with some chemicals required for the experiments.

**Authors' contributions** Keerthana V, Jothika S, Kavitha D and Gopikrishna A have executed the experiments. Agnishwar Girigoswami and Koyeli Girigoswami have given the concept, done experiments and prepared the manuscript. Keerthana V has also prepared the manuscript. Somanathan T has contributed some chemicals and prepared the manuscript.

Funding The study was funded by Council of Scientific and Industrial Research (CSIR), INDIA, Scheme No. 01(2868)/17/EMR-II.

**Availability of data and material** All the authors declare that all data and materials support their published claims and comply with field standards.

#### **Declarations**

Conflict of Interest The authors have no relevant financial or nonfinancial interests to disclose. The authors have no conflicts of interest to declare that are relevant to the content of this article. All authors certify that they have no affiliations with or involvement in any organization or entity with any financial interest or non-financial interest in the subject matter or materials discussed in this manuscript. The authors have no financial or proprietary interests in any material discussed in this article.

Ethical Approval The manuscript is not to be submitted to more than one journal for simultaneous consideration. The submitted work is original and should not have been published elsewhere in any form or language (partially or in full). A single study is not split up into several parts to increase the quantity of submissions and submitted to various journals or to one journal over time (i.e., 'salami-slicing/publishing'). Results are presented clearly, honestly, and without fabrication, falsification or inappropriate data manipulation (including image-based manipulation). Authors have adhered to discipline-specific rules for acquiring, selecting and processing data. No data, text, or theories by others are presented as if they were the author's own ('plagiarism'). Proper acknowledgements to other works have been given.

Informed Consent Not applicable.



#### References

- Akhtar N, Metkar SK, Girigoswami A, Girigoswami K (2017) ZnO nanoflower based sensitive nano-biosensor for amyloid detection. Mater Sci Eng C 78:960–968
- Al-Musawi TJ, Arghavan SMA, Allahyari E et al (2022) Adsorption of malachite green dye onto almond peel waste: a study focusing on application of the ANN approach for optimization of the effect of environmental parameters. Biomass Conv Bioref. https://doi.org/10.1007/s13399-021-02174-6
- Amini M, Younesi H, Bahramifar N, Akbar A, Lorestani Z, Ghorbani F, Daneshi A, Sharifzadeh M (2008) Application of response surface methodology for optimization of lead biosorptioninan aqueous solution by *Aspergillusniger*. J Hazard Mater 154:694–702
- Awang H, Talalah N (2019) Synthesis of reduced graphene oxidetitanium (rGO-TiO<sub>2</sub>) composite using a solvothermal and hydrothermal methods and characterized via XRD and UV–Vis. Nat Resour 10:17–28. https://doi.org/10.4236/nr.2019. 102002
- Deepika R, Girigoswami K, Murugesan R, Girigoswami A (2018) Influence of divalent cation on morphology and drug delivery efficiency of mixed polymer nanoparticles. Curr Drug Deliv 15(5):652–657
- Desai C, Jain KR, Boopathy R, van Hullebusch ED, Madamwar D (2021) Eco-sustainable bioremediation of textile dye wastewaters: innovative microbial treatment technologies and mechanistic insights of textile dye biodegradation. Front Microbiol 2021:12
- Elazab HA, Gadalla MA, Sadek MA, El-Idreesy TT (2019) Hydrothermal synthesis of graphene supported Pd/Fe3O4 nanoparticles as efficient magnetic catalysts for Suzuki Cross-Coupling. Biointerface Res Appl Chem 9(2):3906–3911. https:// doi.org/10.33263/BRIAC92.906911
- Giovannetti R, Rommozzi E, Zannotti M, Anna D'Amato C (2017) Recent advances in graphene based TiO<sub>2</sub> nanocomposites (GTiO<sub>2</sub>Ns) for photocatalytic degradation of synthetic dyes. Catalysts 7:305
- Girigoswami K, Viswanathan M, Murugesan R, Girigoswami A (2015) Studies on polymer-coated zinc oxide nanoparticles: UVblocking efficacy and in vivo toxicity. Mater Sci Eng C 56:501–510
- Girigoswami A, Ramalakshmi M, Akhtar N, Metkar SK, Girigoswami K (2019) ZnO Nanoflower petals mediated amyloid degradation—an in vitro electrokinetic potential approach. Mater Sci Eng C 101:169–178
- Jeyasubramanian K, Muthuselvi M, Hikku GS, Muthusankar E (2019) Improving electrochemical performance of reduced graphene oxide by counteracting its aggregation through intercalation of nanoparticles. J Colloids Interface Sci 549:22–32
- Khanvirdiloo S, Ziamajidi N, Moradi A et al (2021) Effects of vitamins A and E on TiO<sub>2</sub> nanoparticles-induced spermatogenesis defects in male Wistar Rats. Iran J Sci Technol Trans Sci 45:1191–1200. https://doi.org/10.1007/s40995-021-01114-3
- Leary R, Westwood A (2011) Carbonaceous nanomaterials for the enhancement of  $TiO_2$  photocatalysis. Carbon 49:741–772
- Lellis B, Fávaro-Polonio CZ, Pamphile JA, Polonio JC (2019) Effects of textile dyes on health and the environment and bioremediation potential of living organisms. Biotechnol Res Innov 3(2):275–290
- Linley S, Liu Y, Ptacek CJ, Blowes DW, Gu FX (2014) Recyclable graphene oxide-supported titanium dioxide photocatalysts with tunable properties. ACS Appl Mater Interfaces 6(7):4658–4668
- Liu J, Bai H, Wang Y, Liu Z, Zhang X, Sun DD (2010) Self-assembling TiO<sub>2</sub> nanorods on large grapheme oxide sheets at a

- two-phase interface and their anti-recombination in photocatalytic applications. Adv Funct Mater 20:4175–4181
- Mittal A, Mittal J, Malviya A, Kaur D, Gupta VK (2010) Adsorption of hazardous crystal violetfrom waste water by waste materials. J Colloid Interface Sci 343:463–473
- Nelson CR, Hites RA (1980) Aromatic amines in and near the Buffalo River. Environ Sci Technol 14(9):1147–1149
- Obodo RM, Ahmad I, Ezema FI (2019) Introductory chapter: graphene and its applications. In: Ahmad I, Ezema FI (eds) Graphene and its derivatives—synthesis and applications. IntechOpen. https://doi.org/10.5772/intechopen.86023
- Raliya R, Avery C, Chakrabarti S, Biswas P (2017) Photocatalytic degradation of methyl orange dye by pristine titanium dioxide, zinc oxide, and graphene oxide nanostructures and their composites under visible light irradiation. Appl Nanosci 7(5):253–259
- Ram C, Pareek RK, Singh V (2012) Photocatalytic degradation of textile dye by using titanium dioxide nanocatalyst. Int J Theor Appl Sci 4(2):82–88
- Rosu M-C, Coros M, Pogacean F, Magerusan L, Socaci C, Turza A, Pruneanu S (2017) Azo dyes degradation using TiO<sub>2</sub>-Pt/graphene oxide and TiO<sub>2</sub>-Pt/reduced graphene oxide photocatalysts under UV and natural sunlight irradiation. Solid State Sci. https://doi.org/10.1016/j.solidstatesciences.2017.05.013
- Scarpelli F, Mastropietro TF, Poerio T, Godbert N (2018) Mesoporous TiO<sub>2</sub> thin films: state of the art. In: Yang D (ed) Titanium dioxide—material for a sustainable environment. IntechOpen. https://doi.org/10.5772/intechopen.74244. Available from: https://www.intechopen.com/chapters/59572
- Senthilkumaar S, Kalaamani P, Subburaam CV (2006) Liquid phase adsorption of crystal violet onto activated carbons derived from male flowers of coconut tree. J Hazard Mater 136(3):800–808
- Shariatzadeh Bami S, Khavari-Nejad RA, Ahadi AM et al (2021) TiO<sub>2</sub> nanoparticles effects on morphology and physiology of *Artemisia absinthium* L. under salinity stress. Iran J Sci Technol Trans Sci 45:27–40. https://doi.org/10.1007/s40995-020-00999-
- Shi J-W, Ai H-Y, Chen J-W, Cui H-J, Fu M-L (2014) The composite of nitrogen-doped anatase titania plates with exposed 001 facets/graphene nanosheets for enhanced visible-light photocatalytic activity. J Colloid Interface Sci 430:100–107
- Somanathan T, Prasad K, Ostrikov KK, Saravanan A, Krishna VM (2015) Graphene oxide synthesis from agro waste. Nanomaterials (basel) 5(2):826–834. https://doi.org/10.3390/nano5020826
- Tayel A, Ramadan AR, El Seoud OA (2018) Titanium dioxide/graphene and titanium dioxide/graphene oxide nanocomposites: synthesis, characterization and photocatalytic applications for water decontamination. Catalysts 8:491
- Vedhantham K, Girigoswami A, Harini A, Girigoswami K (2022) Waste water remediation using nanotechnology—a review. Biointerface Res Appl Chem 12(4):4476–4495
- Venkatachalam N, Palanichamy M, Murugesan V (2007) Sol-gel preparation and characterization of nanosize TiO<sub>2</sub>: its photocatalytic performance. Mater Chem Phys 104:454–459
- Yaseen DA, Scholz M (2019) Textile dye wastewater characteristics and constituents of synthetic effluents: a critical review. Int J Environ Sci Technol 16:1193–1226. https://doi.org/10.1007/s13762-018-2130-z
- Yoo D-H, Cuong TV, Pham VH, Chung JS, Khoa NT, Kim EJ, Hahn SH (2011) Enhanced photocatalytic activity of graphene oxide decorated on TiO<sub>2</sub> films under UV and visible irradiation. Curr Appl Phys 11:805–808
- Zaaba NI, Foo KL, Hashim U, Tan SJ, Liu W-W, Voon CH (2017) Synthesis of graphene oxide using modified hummers method: solvent influence. Proc Eng 184:469–477





- Zhang Y, Tang Z-R, Fu X, Xu Y-J (2010a)  $TiO_2$  graphene nanocomposites for gas phase photocatalytic degradation of volatile aromatic pollutant: is  $TiO_2$  graphene truly different from other  $TiO_2$  carbon composite materials? ACS Nano 4(12):7303-7314
- Zhang H, Lv X, Li Y, Wang Y, Li J (2010b) P25-graphene composite as a high performance photocatalyst. ACS Nano 4:380-386
- Zindani D, Kumar K (2019) Graphene-based polymeric nanocomposites: an introspection into functionalization, processing techniques and biomedical applications. Biointerface Res Appl Chem 9(3):3926–3933. https://doi.org/10.33263/BRIAC93. 926933

